Detection of heart failure-related biomarker in whole blood with graphene field effect transistor biosensor

Yong-Min Lei, Meng-Meng Xiao, Yu-Tao Li, Li Xu, Hong Zhang, Zhi-Yong Zhang, Guo-Jun Zhang

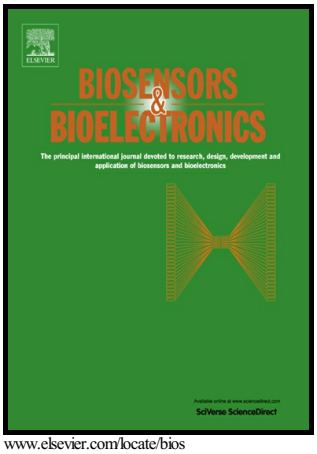

www.elsevier.com/locate/bios

PII: S0956-5663(16)31244-1
DOI: http://dx.doi.org/10.1016/j.bios.2016.12.018
Reference: BIOS9411

To appear in: *Biosensors and Bioelectronic*

Received date: 23 August 2016
Revised date: 5 December 2016
Accepted date: 7 December 2016

Cite this article as: Yong-Min Lei, Meng-Meng Xiao, Yu-Tao Li, Li Xu, Hong Zhang, Zhi-Yong Zhang and Guo-Jun Zhang, Detection of heart failure-related biomarker in whole blood with graphene field effect transistor biosensor *Biosensors and Bioelectronic,* http://dx.doi.org/10.1016/j.bios.2016.12.018

Detection of heart failure-related biomarker in whole blood with graphene field effect transistor biosensor

Yong-Min Lei[1, 2], Meng-Meng Xiao[3], Yu-Tao Li[1], Li Xu[4], Hong Zhang[5], Zhi-Yong Zhang[3,*], Guo-Jun Zhang[1,*]

[1]School of Laboratory Medicine, Hubei University of Chinese Medicine, 1 Huangjia Lake West Road, Wuhan 430065, P.R. China

[2]School of Information Engineering, Wuhan Technology and Business University, 1 Huangjia Lake West Road, Wuhan 430065, P.R. China

[3]Key Laboratory for the Physics and Chemistry of Nanodevices, Department of Electronics, Peking University, No.5 Yiheyuan Road Haidian District, Beijing 100871, P.R. China

[4]School of Pharmacy, Hubei University of Chinese Medicine, 1 Huangjia Lake West Road, Wuhan 430065, P.R. China

[5]Teaching and Research Office of Forensic Medicine, Hubei University of Chinese Medicine, 1 Huangjia Lake West Road, Wuhan 430065, China

[*]Corresponding author: Tel: +86-27-68890259, Fax: +86-27-68890259

E-mail: zhanggj@hbtcm.edu.cn; zyzhang@pku.edu.cn

Abstract

Since brain natriuretic peptide (BNP) has become internationally recognized biomarkers in the diagnosis and prognosis of heart failure (HF), it is highly desirable to search for a novel sensing tool for detecting the patient's BNP level at the early stage. Here we report a platinum nanoparticles (PtNPs)-decorated reduced graphene oxide (rGO) field effect transistor (FET) biosensor coupled with a microfilter system for label-free and highly sensitive detection of BNP in whole blood. The PtNPs-decorated rGO FET sensor was obtained by drop-casting rGO onto the pre-fabricated FET chip and subsequently assembling PtNPs on the graphene surface. After anti-BNP was bound to the PtNPs surface, BNP was successfully detected by the anti-BNP immobilized FET biosensor. It was found that the developed FET biosensor was able to achieve a low detection limitation of 100 fM. Moreover, BNP was successfully detected in human whole blood sample treated by a custom-made microfilter, suggesting the sensor's capability of working in a complex sample matrix. The developed FET biosensor provides a new sensing platform for protein detection, showing its potential applications in clinic sample.

Keywords: Brain natriuretic peptide; Reduced graphene oxide; Platinum nanopa rticles; Human whole blood; Field effect transistor biosensor; Detection

1. Introduction

Cardiovascular disease is the leading cause of death in most countries worldwide (Chen et al., 2012; Finucane et al., 2011; Nguyen et al., 2013, Mensah and Brown, 2007) and one of the most significant clinical manifestations of the disease is heart failure (HF) (Tang et al., 2007). Studies have shown that brain natriuretic peptide (BNP) can rise in the early HF (Palazzuoli et al., 2012; Maisel et al., 2008). BNP is a cardiac hormone that is synthesized predominantly in the heart ventricles (Saito et al., 1989). It has become an internationally recognized biomarker in the diagnosis of HF (Bettencourt, 2004; de Avila et al., 2013; Rezaei et al., 2016), and has great application value and curative effect evaluation in the diagnosis and prognosis of diseases of the cardiovascular system (Mills et al., 2002; Gelfand et al., 1991). One of the most common and dangerous acute cardiovascular presentations among patients reporting to Emergency Departments is acute HF. Currently patients, in whom HF is suspected, undergo diagnostic assessement including medical history, physical examination, electrocardiogram (EKG) and blood tests. The mainstay blood test assisting diagnosis of HF is BNP. Most tests, however, are done in a central laboratory setting and have a turnaround time of 90-120 min. Therefore, there is a need for a reliable, highly sensitive, precise and rapid point-of–care test system allowing measurement of BNP, providing results within minutes of sampling in the Emergency Department.

Now fluorescence immunoassay method is being used to detect BNP in clinical practice. However, this assay is time-consuming (1-4.5 h) and requires fluorescent tags (Liu et al., 2010; Ahmed et al., 2014). Many new methods reported in

laboratories have shown good selectivity and high sensitivity for the past years. For instance, Matsuura et al. (Matsuura et al., 2005) reported a highly sensitive and low-cost immunoassay method for BNP measurement. Three years later, a two-dimensional cross-linked polysiloxane Langmuir-Blodgett film was reported to be useful as a permselective layer in amperometric BNP biosensors (Mizutani, 2008). The dynamic range for BNP was found to be from 13 to 60 pM, but the total assay time was 70 min. In 2012, Lee et al. (Lee et al., 2012) used single site-specific polyaniline nanowire-based biosensors integrated with microfluidic channels to detect very low concentrations of BNP (17 fM). In 2013, Jang et al. (Jang et al., 2014) used surface plasmon resonance (SPR) method for direct detection of BNP with detection limit as low as 1 aM. Despite that many of sensitive biosensors have been built for BNP detection, there were few reports about the BNP measurement in blood or serum samples. Hence, biosensors capable of detecting BNP in whole blood sample with high sensitivity and high specificity are highly desired so that a negative event could be detected even before the patient actually starts feeling badly.

Graphene field effect transistor (G-FET) biosensors have the potentials to meet the aforementioned criteria because of their capability of performing rapid, label-free, electrical detection with potentially low cost, high sensitivity and specificity (Choi et al., 2010). For the past few years, researchers have demonstrated successful detection of metal ions (Sudibya et al., 2011), small molecule (Kwon et al., 2015; Wang et al., 2015), microRNA (Cai et al., 2015; Zhu et al., 2015), DNA (Cai et al., 2014; Zheng et al., 2015), proteins (Zhang et al., 2016; Soikkeli et al., 2016) by using the G-FET-based biosensors. In the meantime, platinum nanoparticles (PtNPs) functionalized graphene and carbon nanotube-based FET biosensors have been already demonstrated for some applications. For instance, Penza et al. (Penza et al.,

2007) fabricated a PtNPs-functionalized multiwalled carbon nanotube (MWCNT) gas sensor for detection of NH_3 and NO_2, respectively. Moreover, Zhang et al. (Zhang et al., 2015) developed PtNPs-functionalized graphene solution-gated transistors, which could be used for sensitive detection of H_2O_2. Yin et al. (Yin et al., 2012) reported PtNPs decorated chemical vapor deposition (CVD)-grown graphene composites FETs for detection of DNA. However, a challenge still remains toward making this technology detectable in whole blood as such complex environments are known to cause problems as false signal and saturation of receptors. Very recently, Wang et al. (Wang et al., 2016) reported a label-free and portable aptasensor based on G-FET for effective children blood lead detection, in which a pre-treatment was needed to add chemical reagents to blood. However, there is no report regarding BNP detection in whole blood by using the G-FET biosensors integrated with a sample pretreatment system.

In this report, we demonstrate a detection system by integrating a custom-made microfilter for removing blood cells with the PtNPs-decorated reduced graphene oxide (rGO) FET biosensor for detecting BNP in human whole blood with high sensitivity and specificity. The PtNPs-decorated rGO FET sensor is obtained by drop-casting rGO onto the pre-fabricated FET chip and assembling PtNPs on the graphene surface. After anti-BNP is bound to the PtNPs surface, BNP is successfully detected by the anti-BNP immobilized FET biosensor. Therefore, the system developed here does not require any added reagents or sophisticated fabrication process, showing a potential for an integrated and portable detection.

2. Experimental Section

2.1. Materials

Na_2PtCl_4, NHS, EDC, BNP and anti-BNP were purchased from Sigma-Aldrich

(shanghai, China). Human serum albumin (HSA), bull serum albumin (BSA), and D-Dimer were purchased from Thalys Co. Ltd. (Wuhan, China). Graphene oxide (GO) powder (99.99995%, 325 mesh) was purchased from Alfa Aesar Co. Ltd. (Tianjin, China). 98% hydrazine, 35 wt % H_2O_2, and other chemicals were purchased from Generay Biotech Co. Ltd. (Shanghai, China). Ultrapure water was obtained from a Millipore water purification system (18.2 MΩ resistivity, Milli-Q Direct 8).

2.2. Fabrication of rGO FET Biosensors

The fabrication of the FET biosensor chip was completed by using the standard semiconductor technology according to our previous reports (Cai et al., 2014; Zhang et al., 2016). 2 mg of the GO powder was put into 1 mL of Milli-Q water, followed by sonication for 1 h, to produce a uniform solution. Then, 1 mL of 98% hydrazine was added and shaked for 1 week for the purpose of thorough reduction of GO. The resulting 1 mg/mL stock solution of rGO could be stable for months without aggregation. The diluted rGO (0.1 mg/mL) suspension was drop-casted onto the sensor array region, and thermally annealed at 150 °C for 2 h in order to remove all hydrazine and enhance the contact between the rGO and the electrodes. After that, the chip was immersed in the Pirahna solution (7:3 v/v concd H_2SO_4/35% H_2O_2) and sonicated for 5 s to obtain few-layer R-GO, followed by thoroughly washing with ethanol and DI water and drying with nitrogen.

2.3. Decoration of platinum nanoparticles

The rGO FET biosensor was immersed in the solution of 2 mL of 5 mM Na_2PtCl_4 solution in the mixed H_2O/ethanol (v:v =1:1) solvent. Then the UV light source was introduced to directly irradiate the biosensor chip. In order to make an efficient and complete reaction for deposition of dense PtNPs (~10 nm) on rGO, the

chip was exposed to the UV light (WD-9403C, Beijing) at 29 W with 368 nm wavelength for 30 min. After washing the chip with ethanol, followed by thoroughly washing with DI water, and drying with nitrogen, the PtNPs-decorated rGO FET was achieved.

2.4. Surface functionalization

In order to immobilize anti-BNP on the PtNPs surfaces, the PtNPs-decorated graphene FET was treated with a 10 mM thioglycolic acid in DI water overnight at room temperature, and washed with DI water, producing carboxylic group on the terminal of the PtNPs surface through Pt-S bond formation. To pre-activate the carboxylic groups, a mixture solution containing 0.4 M EDC and 0.1 M NHS was prepared in equal volume. The chip was soaked in the mixture solution at 4°C for 30 min, after which the chip was thoroughly washed with 1×PBS and DI water. Then 100 μg/ml anti-BNP was introduced to the FET chip and incubated at 4°C overnight. The chip was rinsed in sequence with 1×PBS containing 0.2% SDS, 1×PBS and DI water to remove the unreacted antibody. The chip was then incubated with 1 mg/ml BSA solution for 1 h to prevent possible nonspecific binding events and then rinsed by DI water.

2.5. Immunodetection

Protein immunodetection was conducted by dropping an appropriate concentration of BNP solution onto the device and incubated for 30 min on a shaker at 4°C. Then the chip was rinsed in sequence with 1×PBS containing 0.2% SDS, 1×PBS, and DI water to remove the un-bound biomolecule, then dried with N_2. In this study, a

custom-made microfilter and polycarbonate membranes with 400 nm pores were used to remove blood cells for human blood detection. After filtration, serum containing BNP was delivered onto the rGO FET biosensors and allowed for incubation for 30 min at 4°C for immunoreaction. After that, the chip was then rinsed by 1×PBS and water, respectively, to wash off the un-bound BNP and dried by N_2.

2.6. Measurements

The liquid-gated graphene FET devices were measured in a semiconductor parameter analyzer (Keithley 4200-SCS) coupled with a probe station (EverBeing BD-6). For I_{ds}-V_G curve measurements of the FET devices, a silver wire was used as a gate electrode and a constant bias V_{ds}=0.1 V was applied. 0.001×PBS solution was used in all the measurements. During the real-time sensing experiment, a small source drain voltage V_{ds} (0.1 V) and gate electrode voltage V_G (0.3 V) was applied to the device, and the source drain current Ids was measured and recorded in real time.

2.7. Characterizations

A field emission-scanning electron microscope (FE-SEM) (Zeiss SIGMA, Germany) was used for SEM characterization of the device with an accelerating voltage set at 5 kV. Transmission electron microscopy (TEM) (JEM-2100, Japan) was used for observing the morphology of PtNPs. X-ray Energy Dispersive Spectrum (EDS) was detected by Genesis 2000 xMS (EDAX, USA). X-ray photoelectron spectroscopy (XPS) spectra were employed to confirm PtNPs formation on the rGO surface by an ESCALAB 250Xi XPS (Thermo Fisher, America) and the source gun types were Al and Ka.

3. Results and Discussion

3.1. Detection principle

Fig. 1 illustrates the detection system of the PtNPs-decorated rGO FET biosensor and a custom-made microfilter for BNP detection in whole blood. First, a diluent rGO solution is drop-casted onto the channel of the sensor chip as the conducting material. Then PtNPs are decorated on the rGO surface through photochemical synthesis upon immersion of the chips in Na_2PtCl_4 solution under UV light (Cameron and Bocarsly, 1985; Yin et al., 2012). PtNPs as metal nanoparticles can help amplify the sensor's electrical signal (Li et al., 2015(a); Li et al., 2015(b); Zhai et al., 2013). After thioglycolic acid is modified on the PtNPs surface through Pt-S bonding, BNP antibody molecule can be covalently immobilized on the PtNPs surface through the well-known carbodiimide coupling reaction provided by an 1-ethyl-3-(3-dimethylaminopropyl) carbodiimidehydrochloride/N-hydroxysuccinimide (EDC/NHS) system (Länge et al., 2003; Lewis et al., 1994). The details of the functional process are shown in Fig. S1. BNP in the whole blood treated by custom-made microfilter is measured by immunoreaction with the immobilized BNP antibody. In the setup, a silver wire is used as the reference electrode to realize liquid-gated FET for electrical measurements.

3.2. Characterizations

Aiming to increase the conductivity and electrical response signals, PtNPs were directly synthesized on the rGO film by immersion of rGO FET chip in an aqueous

ethanolic solution of 5 mM Na_2PtCl_4, followed by UV light irradiation. Then the $PtCl_4^{-2}$ could be photochemically reduced to Pt^0 in the presence of alcohols (Cameron and Bocarsly, 1986; Cameron and Bocarsly, 1985; Yin et al., 2012). As shown in Fig. 2A, a continuous and few-layer rGO film and PtNPs on the rGO surface were obviously seen by SEM. Controlling of the illumination time of UV light could generate dense PtNPs in the size of ～10 nm on the rGO surface, which were clearly visible in Fig. 2A (Inset). As seen in Fig. S2, TEM was also conducted to verify the size of PtNPs. PtNPs formation on the rGO surface was further confirmed by EDS, as shown in Fig. S3. The peak at 2.2 keV was attributed to the M_α-M_β and M_γ characteristic peaks of Pt (Donev and Hastings, 2009). The detected C and O peaks were mainly from rGO, and the Si peak was mainly from the silicon chip substrate.

In order to prove that the UV method was effective in the reduction of platinum precursor, XPS analysis was carried out after dense PtNPs were conjugated on the rGO surface. As seen from Fig. S4, double peaks were observed at 71.7 and 75.2 eV (black line), which were attributable to $4f_{7/2}$ and $4f_{5/2}$ of metallic Pt, respectively. The results are in good agreement with the previously published paper (Fang et al. 2011; Pietron et al. 2012). Pt 4f could be fitted with three chemical states, as Pt (0) at 71.4 eV, Pt (II) at 72.3 eV, and Pt (IV) at 74.4 eV, respectively. It is clearly observed that the composition of Pt (0) was larger than that of Pt (II) and Pt (IV), indicating that the dominant valence of the Pt species on the rGO was Pt (0). This result suggests that the Na_2PtCl_4 aqueous ethanolic solution followed by UV light irradiation is highly efficient for the preparation of dense PtNPs on the rGO surface.

To prove that the stepwise functionalization process was successful as anticipated, the transfer curves of the G-FET were obtained. The transfer characteristic curves of the G-FET before and after BNP binding were characterized in Fig. 2B. After the rGO film, PtNPs, anti-BNP, and BNP were applied to the FET biosensor surface, I_{ds}-V_G (I_{ds} is the drain-source current, V_G is the gate voltage) graphs were measured, respectively. Similar ambipolar natures were observed for all steps. The modification of PtNPs on the rGO channel resulted in an obvious increase of current as compared with the pristine rGO. It can be attributed to the increased active surface area of the well distributed PtNPs, which promotes the electron transfer between rGO and electrode (Ren et al., 2014). The Dirac point was found to be almost unchanged and be around 0.36 V, which is consistent with Yin's work (Yin et al., 2012). However, it was found that the metal nanoparticles increased the current carrier concentration and enhanced the response of current signal after PtNPs decoration. PtNPs resulted in a covalent immobilization of anti-BNP molecules onto the surface of rGO, not only provides the higher surface area for the conjugation of antibody but also facilitates the electron transfer (Roushani and Valipour, 2016).

Because the isoelectric point (pI) of anti-BNP is estimated to be in the range between 6.6-7.2 (Hamilton et al., 1987), anti-BNP is negatively charged in pH 7.4 PBS solution. When anti-BNP was immobilized on the PtNPs surface through Pt-S bond, the negatively charged anti-BNP would increase negative charge density on the rGO and result in left-shifted Dirac point (0.32 V). The theoretical pI of BNP is 10.95, which was calculated according to Gundry's study (Gundry and Van Eyk, 2007). It is

clear that BNP is positively charged in the buffer solution (pH 7.4). Upon binding to the anti-BNP-immobilized rGO FET biosensor, BNP gave rise to a decrease of net carrier density, resulting in p-doping of the FET. This induced a positive shift of the V_{CNP} in transfer curves. After BNP binding, Dirac point shifted from 0.32 to 0.4 V. The shift of Dirac point is similar to that previously reported (Kim et al., 2013).

3.3. Stability and reproducibility

Firstly, the stability of the PtNPs-decorated rGO FET biosensors was evaluated by storing the functionalized device in a vacuum oven for a period of times and using it for the detection of 200 nM BNP. As shown in the Fig. 3A, the shift of the dirac voltage retained more than 85% of its original value over one week. Signal response slightly decreased as a function of the storing time. This signal decrease is probably because of nonspecific surface adsorptions caused by air and water in environment.

Secondly, to investigate the reproducibility, the anti-BNP immobilized FET biosensor was used for BNP detection over 3 cycles. High ionic solution (NaCl, 1M) was used to dissociate the binding between BNP and anti-BNP, after which regeneration was then realized by re-applying BNP to the anti-BNP immobilized FET biosensor (Duan et al., 2012; Rahim et al., 2013). During 3 cycles, the transfer characteristic curves were repeatedly measured to obtain the gate voltage shift. The shift in gate potential of dirac point was observed between 70 mV and 80 mV during 3 cycles of association and dissociation, indicating that the FET biosensor had the capability of regeneration. These oscillations of the gate potential of dirac point caused by 3 cycleswere shown in Fig. 3B. The results indicate that the functionalized

PtNPs-decorated rGO FET biosensor is sufficiently stable and reproducible.

3.4. Selectivity

To challenge the G-FET biosensor with nonspecific proteins, selectivity test was carried out by using other proteins including BSA, D-Dimer and HSA as control. Various solutions including BSA, D-Dimer, HSA, BNP, BNP+BSA, BNP+D-Dimer and BNP+HSA at the same concentration (100 nM) were prepared in PBS, respectively. The different solutions were incubated with the anti-BNP-immobilized PtNPs-decorated rGO FET biosensors for 30 min, respectively, after which transfer characteristic curves were measured before and after the decoration. ΔV_{CNP} is normalized by the following formula: $\Delta V_{CNP}=V_{CNP\ after\ incubation}-V_{CNP\ before\ incubation}$. When solutions only containing non-target proteins (BSA, D-Dimer and HSA) were applied to the devices, the observed ΔV_{CNP} (11.5±2.0, 13.2±3.7, 17.3±2.8 mV) was much smaller than that obtained from target proteins (BNP)(70.4±7.2 mV) at same concentration，as shown in Fig. 4. The ΔV_{CNP} of the mixed solutions including BNP+BSA, BNP+D-Dimer and BNP+HAS were about 68.0±7.7, 75.0±4.9 and 79.5±4.2 mV, respectively, meaning that BNP could be detectable even in a mixture with other interfering proteins. Such a great selectivity can be attributed to the preferential binding of anti-BNP to BNP over other proteins.

3.5. Sensitivity

The sensitivity of the PtNPs-decorated rGO FET biosensor was examined by challenging it with a series of concentrations of BNP. The real-time response of the sensor upon injection of various concentrations of BNP at constant V_{ds} (0.1 V) and V_G

(0.3 V) was illustrated in Fig. 5A. Known concentrations of BNP in buffer were added after a stable reading using 0.001×PBS buffer was obtained. The sensor showed a very fast real-time response (10 s) when the sensor device was exposed to the diverse concentrations of the target BNP solution. Furthermore, the sensor showed a concentration-dependent decrease in I_{ds} on exposure to BNP solution. The current decrease was caused by the positive charge of the specific target BNP bound to the surface-immobilized anti-BNP. The specific binding caused a structural re-arrangement of the charge distribution, finally leading to a decrease in the negatively charged base state. The decreased negative charge density at the sensor interface could reduce the hopping rate of charge carriers (holes), which is probably responsible for the decrease in current (Bishop et al., 2008). As shown in the Inset, the biosensor could reliably detect BNP down to 100 fM based on the signal that exceeds the background by 3 times.

As shown in Fig. 5B, current signal decreased with the BNP concentration increase. The logarithmic value of BNP concentration defined as lgC showed a linear response within the range of 100 fM-1 nM (Inset). The linear relationship was represented by $\triangle I(nA)= -10.43 lgC_{BNP}(M) -140.40$ and correlation coefficient was 0.9917. Error bars represent standard deviations of measurements (n=3). In general, the greater the BNP level in the blood, the more severe the heart failure condition. The blood BNP concentration under normal conditions is ~6 pM, and it increases to ~600 pM for people potentially going to be HF (Dao et al., 2001; Jang et al., 2015; Seino et al., 2004). So the result reveals that the FET biosensor could achieve high

sensitivity, which is capable of detecting BNP in human whole blood at the early stage of HF.

The performance comparison among various BNP biosensors was listed in Table S1. In clinical tests, Elisa test kit was used for BNP detection and the sensitivity as high as 5 pM could be achieved (Ahmed et al., 2014). Matsuura et al. (Matsuura et al., 2005) used an electrochemical enzyme immunoassay method for BNP detection with a detection sensitivity of 3 pM. Kurita et al. (Kurita et al., 2006) reported a surface plasmon resonance (SPR) method for BNP detection and they obtained a detection limit down to 1 pM. Mizutani et al. (Mizutani, 2008) utilized a two-dimensional cross-linked polysiloxane Langmuir-Blodgett film in amperometric biosensors for BNP detection with a sensitivity of 13 pM. Lee et al. (Lee et al., 2012) used single site-specific polyaniline nanowire-based biosensors integrated with microfluidic channels to detect BNP with detection limit of 17 fM. Prasad et al. (Prasad et al., 2013) developed a silicon nanosensor based on electrical impedance measurements for the detection of BNP with very low detection limit down to 0.3 aM. The sensitivity of the PtNPs-decorated rGO FET biosensor reported in the work is higher than that reported by Elisa, electrochemical method, and SPR, but lower than that reported by nanowire and silicon nanosensor. Although the sensitivity is not the highest, the fabricated PtNPs-decorated rGO FET biosensor can be used for diagnosis of early heart failure.

3.6. BNP detection in whole blood

To the best of our knowledge, none of them was used for the measurement of

BNP in real blood sample although many graphene-based FET biosensors have been reported. To address this challenging issue, the feasibility of the FET biosensor for measuring BNP in human blood samples was tested. Healthy human blood samples were collected from Wuhan No.1 Hospital (Wuhan, China). To demonstrate the detection capability in whole blood, BNP was spiked into healthy human blood, and different concentrations of BNP in blood were prepared. Due to the complexity in blood, especially blood cells, pre-treatment was required prior to BNP detection. It is essential that an integrated system is expected, which can make the measurement portable. To this end, the custom-made microfilter was employed to remove blood cells. After that, the serum was dropped onto the anti-BNP-immobilized FET biosensor. The testing results of the FET biosensor with three different concentrations (50 nM, 100 nM, 200 nM) of BNP in blood were shown in Fig. 6A. As a control, only serum as the blank solution was delivered onto the PtNPs-decorated rGO FET biosensors and incubated for 20 min at 4 °C. The V_{CNP} was almost unchangeable and kept around 0.32 V, indicating that serum excluding BNP does not cause binding of non-specific proteins to the FET surface. After blood solutions including 50, 100, 200 nM BNP, respectively, were filtered and applied to the FET biosensors, it was clearly observed that right shift of the transfer curves occurred and the ΔV_{CNP} was 44, 58, 73 mV, respectively. Higher concentrations of BNP in blood, larger shifts of V_{CNP}. To compare the performance capabilities of the different FET biosensors, the two representative FET biosensors were interacted with different concentrations of BNP in the tested blood. The corresponding shift of V_{CNP} were summarizes in Fig. 6B. It was

seen that the two different devices showed the similar performance and the response increased along with the increase of BNP concentrations in blood, clearly demonstrating the FET's ability to detect biomarkers in human blood sample.

4. Conclusions

In summary, we have demonstrated a label-free and highly sensitive protein biosensor based on the PtNPs-decorated rGO FET, which has the capability of detecting BNP in the real blood sample by integrating with a custom-made microfilter. The PtNPs-decorated rGO FET sensor increased the electrical conductivity after PtNPs decoration. Thus, the PtNPs-decorated rGO FET sensors could specifically detect BNP and achieve a detection limit as low as 100 fM. Moreover, BNP was successfully detected by the FET biosensor in human whole blood sample treated by the custom-made microfilter. The results demonstrate that the developed FET biosensor shows potentials of integration and portability, which is applicable for early detection and prognostic evaluation in HF patients.

Acknowledgements

This work was supported by the National Natural Science Foundation of China (Nos. 21275040, 21475034, 21675041 and 61390504).

Supporting Information

Supplementary data associated with this article can be found in the online version at …

References

Ahmed F. A., Ferial A. A. M., Abdul-Karim Y. A. S., 2014. Iraqi Journal of Science 55, 1541-1546.

Bettencourt, P., 2004. Eur. J. Heart Fail. 6, 359-363.

Bishop, J., Chagovetz, A. M. & Blair, S., 2008. Biophys. J. 94, 1726-1734.

Cai, B., Huang, L., Zhang, H., Sun, Z., Zhang, Z., Zhang, G. J., 2015. Biosens. Bioelectron. 74, 329-334.

Cai, B., Wang, S., Huang, L., Ning, Y., Zhang, Z., Zhang, G. J., 2014. ACS nano 8, 2632-2638.

Cameron, R. E., Bocarsly, A. B., 1985. J. Am. Chem. Soc. 107, 6116-6117.

Cameron, R. E., Bocarsly, A. B., 1986. Inorg. Chem. 25, 2910-2913.

Chen, Z., Yang, G., Offer, A., Zhou, M., Smith, M., Peto, R., Ge, H., Yang, L., Whitlock, G., 2012. Int. J. Epidemiol. 41, 472-481.

Choi, W., Lahiri, I., Seelaboyina, R., Kang, Y. S., 2010. Critical Reviews in Solid State and Materials Sciences 35, 52-71.

Dao, Q., Krishnaswamy, P., Kazanegra, R., Harrison, A., Amirnovin, R., Lenert, L., Clopton, P., Alberto, J., Hlavin, P., Maisel, A. S., 2001. J. Am. Coll. Cardiol. 37, 379-385

de Avila, B. E., Escamilla-Gomez, V., Campuzano, S., Pedrero, M., Pingarron, J. M. , 2013. Anal. Chim. Acta, 784, 18-24.

Duan, X., Li, Y., Rajan, N. K., Routenberg, D. A., Modis, Y., Reed, M. A., 2012. Nat. Nanotechnol. 7, 401-407.

Donev, E. U., Hastings, J. T., 2009. Nano Lett. 9, 2715-2718.

Fang, B., Kim, M. S., Kim, J. H., Song, M. Y., Wang, Y. J., Wang, H., Wilkinson, D. P., Yu, J. S., 2011. J. Mater. Chem. 21, 8066-8073.

Finucane, M. M., Stevens, G. A., Cowan, M. J., Danaei, G., Lin, J. K., Paciorek, C. J., Singh, G. M., Gutierrez, H. R., Lu, Y., Bahalim, A. N., Farzadfar, F., Riley, L. M., Ezzati, M., Global Burden of Metabolic Risk Factors of Chronic Diseases Collaborating Group. 2011. Lancet 377, 557-567.

Gelfand, R. A., Frank, H. J., Levin, E., Pedram, A., 1991. Am. J. Physiol. 261, E183-189.

Gundry, R. L., Van Eyk, J. E., 2007. Clin. Chem. 53, 1181-1182.

Hamilton, R. G., Roebber, M., Reimer, C. B., Rodkey, L. S., 1987. Electrophoresis 8, 127-134.

Jang, H. J., Ahn, J., Kim, M. G., Shin, Y. B., Jeun, M., Cho, W. J., Lee, K. H., 2015. Biosens. Bioelectron., 64, 318-323.

Jang, H. R., Wark, A. W., Baek, S. H., Chung, B. H., Lee, H. J., 2014. Anal. Chem. 86, 814-819.

Kim, D. J., Sohn, I. Y., Jung, J. H., Yoon, O. J., Lee, N. E., Park, J. S., 2013. Biosens. Bioelectron. 41, 621-626.

Kurita, R., Yokota, Y., Sato, Y., Mizutani, F., Niwa, O., 2006. Anal. Chem. 78, 5525-5531.

Kwon, O. S., Song, H. S., Park, S. J., Lee, S. H., An, J. H., Park, J. W., Yang, H., Yoon, H., Bae, J., Park, T. H., Jang, J., 2015. Nano Lett. 15, 6559-6567.

Länge, K., Bender, F., Voigt, A., Gao, H., Rapp, M., 2003. Anal. Chem. 75, 5561-5566.

Lee, I., Luo, X., Huang, J., Cui, X. T., Yun, M., 2012. Biosensors 2, 205-220.

Lewis, M. R., Raubitschek, A., Shively, J. E., 1994. Bioconjug. Chem. 5, 565-576.

[a]Li, L., Wang, Y., Pan, L., Shi, Y., Cheng, W., Shi, Y., Yu, G., 2015. Nano Lett. 15, 1146-1151.

[b]Li, L., Shi, Y., Pan, L., Shi, Y., Yu, G., 2015. J. Mater. Chem. B 3, 2920-2930.

Liu, R., Liu, J., Xie, L., Wang, M., Luo, J., Cai, X., 2010. Talanta 81, 1016-1021.

Maisel, A., Mueller, C., Adams, K., Jr., Anker, S. D. et al., 2008. Eur. J. Heart Fail. 10, 824-839.

Matsuura, H., Sato, Y., Niwa, O., Mizutani, F., 2005. Anal. Chem. 77, 4235-4240.

Mensah, G. A., Brown, D. W., 2007. Health affairs 26, 38-48.

Mills, R. M., Hobbs, R. E., Young, J. B., 2002. Congestive heart failure 8, 270-273.

Mizutani, F., 2008. Sens. Actuators B. Chem. 130, 14-20.

Nguyen, H. N., Fujiyoshi, A., Abbott, R. D., Miura, K., 2013. Circ. J. 77, 2851-2859.

Palazzuoli, A., Beltrami, M., Pellegrini, M., Nuti, R., 2012. Clin. Chim. Acta. 413, 1832-1838.

Penza, M., Cassano, G., Rossi, R., Alvisi, M., Rizzo, A., Signore, M. A., Dikonimos, Th., Serra, E., Giorgi, R., 2007. Appl. Phys. Lett. 90, 173123.

Pietron, J. J., Pomfret, M. B., Chervin, C. N., Long, J. W., Rolison, D. R., 2012. J. Mater. Chem. 22, 5197-5204.

Prasad, S., Selvam, A. P., Reddy, R. K., Love, A., 2013. J. Lab. Autom. 18, 143-151.

Rahim, R. A., Tanabe, K., Ibori, S., Wang, X., Kawarada, H., 2013. Biosens. Bioelectron. 40, 277-282.

Ren, F., Wang, H., Zhai, C., Zhu, M., Yue, R., Du, Y., Yang, P., Xu, J., Lu, W., 2014. ACS Appl. Mater. Interfaces 6, 3607-3614.

Rezaei, B., Ghani, M., Shoushtari, A. M., Rabiee, M., 2016. Biosens. Bioelectron. 78, 513-523.

Roushani, M., Valipour, A., 2016. Sens. Actuators B. Chem. 222, 1103-1111.

Saito, Y., Nakao, K., Itoh, H., Yamada, T., Mukoyama, M., Arai, H., Hosoda, K., Shirakami, G., Suga, S., Minamino, N. et al., 1989. Biochem. Biophys. Res. Commun. 158, 360-368.

Seino, Y., Ogawa, A., Yamashita, T., Fukushima, M., Ogata, K., Fukumoto, H., Takano, T., 2004. Eur. J. Heart Fail. 6(3), 295-300.

Soikkeli, M., Kurppa, K., Kainlauri, M., Arpiainen, S., Paananen, A., Gunnarsson, D., Joensuu, J. J., Laaksonen, P., Prunnila, M., Linder, M. B., Ahopelto, J., 2016. ACS Appl. Mater. Interfaces 8, 8257-8264.

Sudibya, H. G., He, Q., Zhang, H., Chen, P., 2011. ACS nano 5, 1990-1994.

Tang, W. H., Francis, G. S., Morrow, D. A., Newby, L. K., Cannon, C. P., Jesse, R. L., Storrow, A. B., Christenson, R. H., Apple, F. S., Ravkilde, J., Wu, A. H., National Academy of Clinical Biochemistry Laboratory Medicine, 2007. Circulation 116, e99-109.

Wang, C., Cui, X., Li, Y., Li, H., Huang, L., Bi, J., Luo, J., Ma, L. Q., Zhou, W., Cao, Y., Wang, B., Miao, F., 2016. Sci. Rep. 6, 21711.

Wang, D., Hu, W., Xiong, Y., Xu, Y., Li, C. M., 2015. Biosens. Bioelectron. 63, 185-189.

Yin, Z., He, Q., Huang, X., Zhang, J., Wu, S., Chen, P., Lu, G., Chen, P., Zhang, Q., Yan, Q., Zhang, H., 2012. Nanoscale 4, 293-297.

Zhai, D., Liu, B., Shi, Y., Pan, L., Wang, Y., Li, W., Zhang, R. Yu, G., 2013. ACS Nano 7, 3540-3546.

Zhang, C., Xu, J. Q., Li, Y. T., Huang, L., Pang, D. W., Ning, Y., Huang, W. H., Zhang, Z., Zhang, G. J., 2016. Anal. Chem. 88, 4048-4054.

Zhang, M., Liao, C., Mak, C. H., You, P., Mak, C. L., Yan, F., 2015. Sci. Rep. 5, 8311-8315.

Zheng, C., Huang, L., Zhang, H., Sun, Z., Zhang, Z., Zhang, G. J., 2015. ACS Appl. Mater. Interfaces 7, 16953-16959.

Zhu, X., Shen, Y., Cao, J., Yin, L., Ban, F., Shu, Y., Li, G., 2015. Chem. Commun. 51, 10002-10005.

Figure captions:

Figure 1. Schematic illustration of the PtNPs-decorated rGO FET biosensor with a custom-made microfilter for BNP detection.

Figure 2. (A) SEM image of photochemically synthesized PtNPs on the rGO film spanning across gold electrodes.(B) Plots of transfer curves at V_{ds}=100 mV for the FET biosensor in the process of rGO formation, PtNPs decoration, anti-BNP immobilization and BNP binding.

Figure 3. (A) Stability test for the PtNPs-decorated rGO FET biosensor over one week. (B) Reproducibility for BNP detection. The shift in gate potential of dirac point was observed at V_{ds}=0.1 V. The concentrations of BNP and NaCl were 200 nM and 1 M, respectively.

Figure 4. Shift of V_{CNP} of the anti-BNP immobilized G-FET biosensor interacted with different proteins at the same concentration.

Figure 5. (A) Real-time electrical detection at different concentrations of BNP solution in PBS (12.5 nM, 25 nM, 50 nM, 100 nM, 200 nM, 400 nM, 800nM). Inset: Real-time electrical detection at lower concentrations of BNP. (B) The response of the PtNPs-decorated rGO biosensors to BNP at a series of concentrations. Inset: The response of the biosensors to BNP at low concentration range (100 fM, 1 pM, 10 pM, 100 pM, 1 nM).

Figure 6. Electrical response of the PtNPs-decorated rGO FET biosensor to different concentrations of BNP in real blood samples. (A) Transfer curves of the PtNPs-decorated rGO FET biosensor interacted with PBS and varying concentrations

of BNP. (B) Shift of V_{CNP} of the two representative devices interacted with PBS and varying concentrations BNP (50 nM, 100 nM, 200 nM), respectively. Error bars show the standard deviations of measurements taken from at least three independent samples.

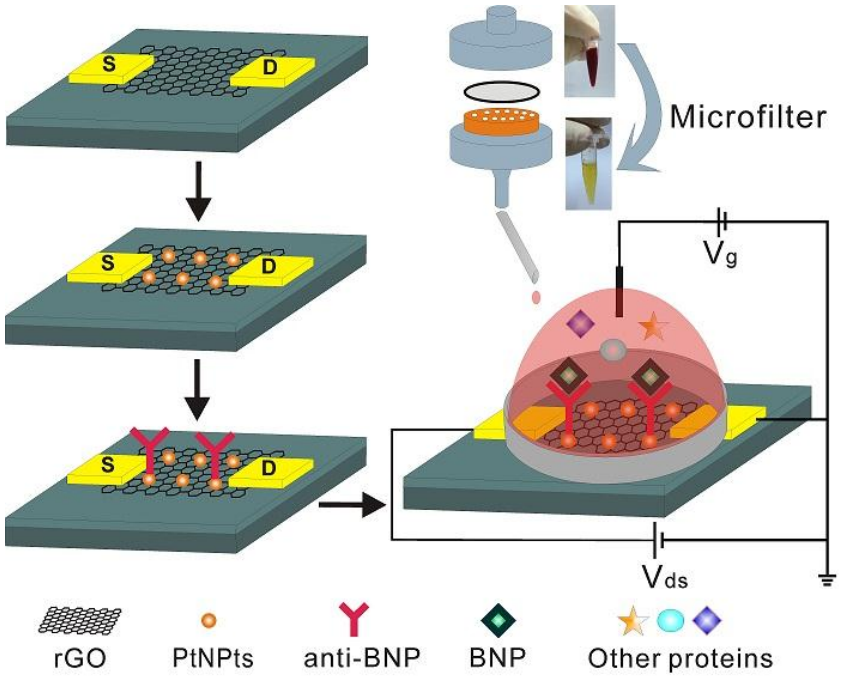
S
D
S
D
S
D
Microfilter
Vg
Vds
rGO
PtNPts
anti-BNP
BNP
Other proteins

Figure 1

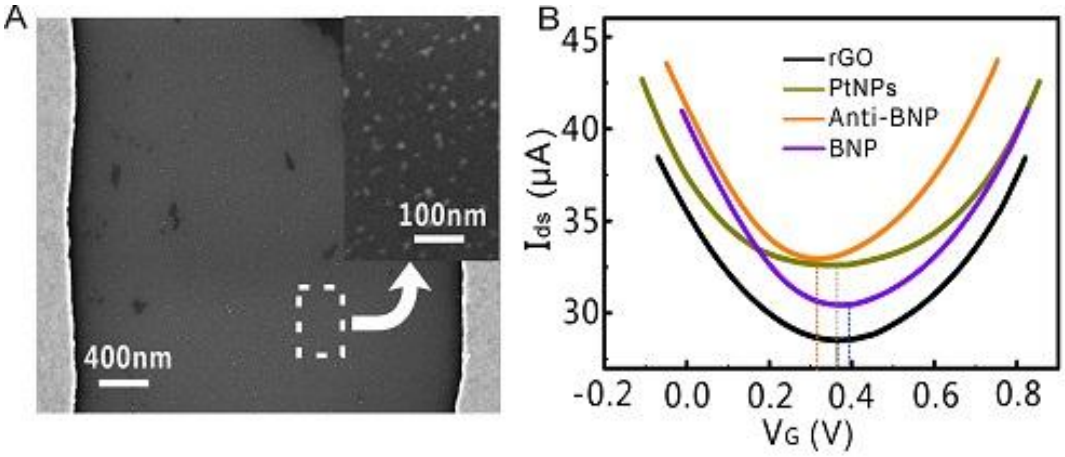

Figure 2

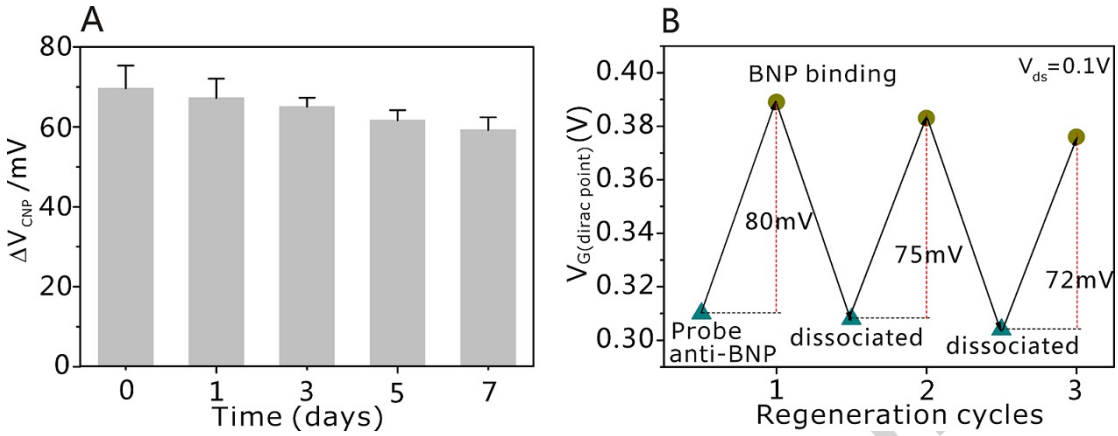

Figure 3

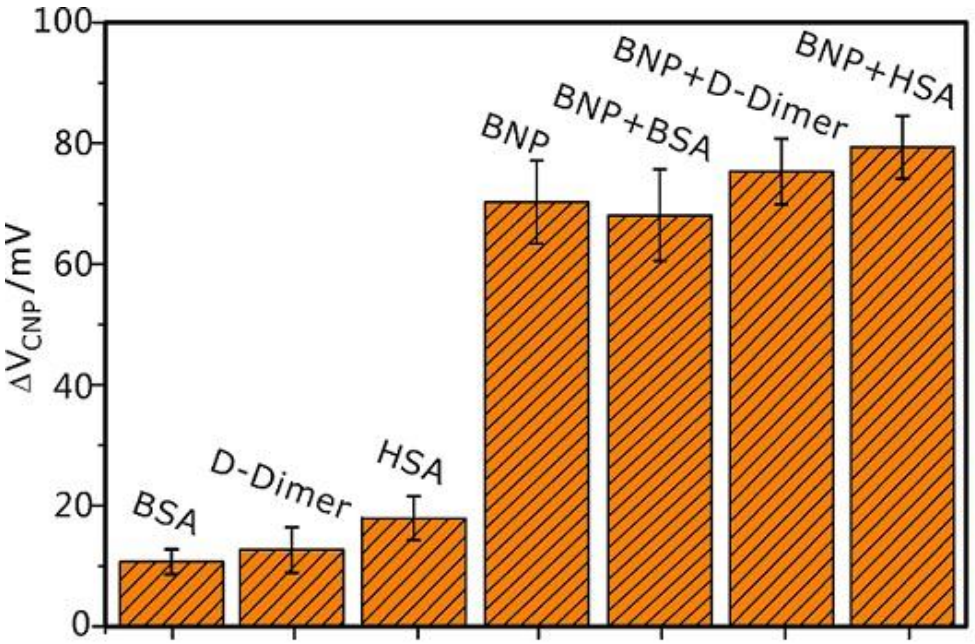

Figure 4

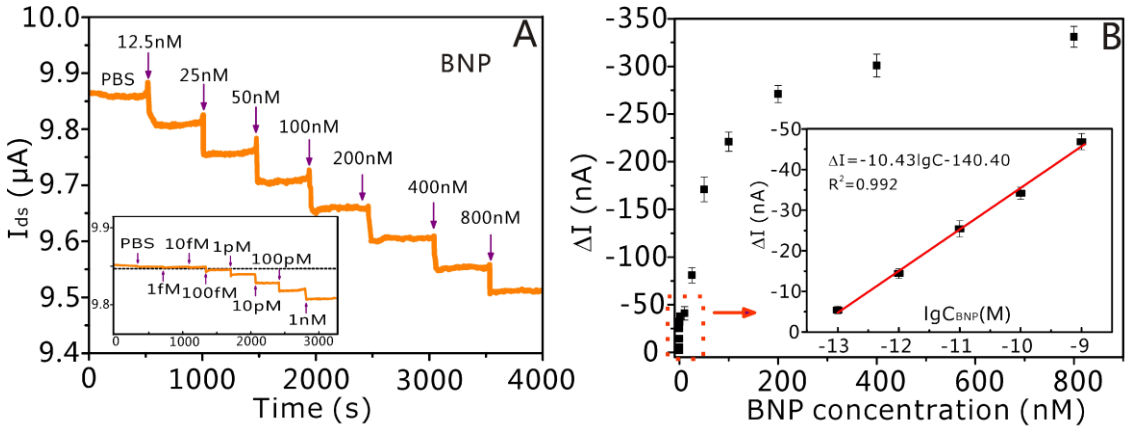

Figure 5

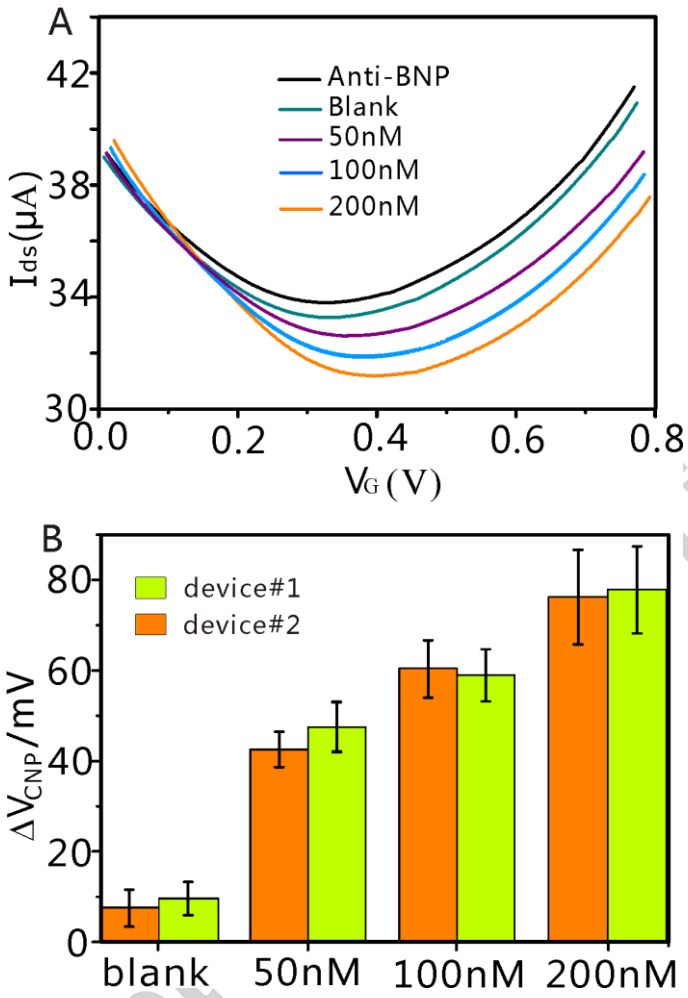
A
42
38
34
30
I_{ds}(μA)
0.0
0.2
0.4
0.6
0.8
V_G (V)
Anti-BNP
Blank
50nM
100nM
200nM
B
80
60
40
20
0
ΔV_{CNP}/mV
device#1
device#2
blank
50nM
100nM
200nM

Figure 6

Highlights

1. For the first time, the PtNPs-decorated graphene FET biosensor coupled with a microfilter system for BNP detection in whole blood has been proposed.
2. Antibody-antigen interaction has been employed to realize the sensitive and specific detection of BNP by using the fabricated FET biosensor.
3. The fabricated FET biosensor is able to detect BNP in real blood sample.
4. High sensitivity has been achieved based on this detection system.
5. The developed sensing platform shows satisfactory specificity.
6. It is an important attempt to explore new detection method for proteins based on graphene FET biosensor.